The Effect of Phosphodiesterase inhibitor on browning of adipose tissue in mice model

Da Hea Seo

Department of Medicine

The Graduate School, Yonsei University

The Effect of Phosphodiesterase inhibitor on browning of adipose tissue in mice model

Da Hea Seo

Department of Medicine

The Graduate School, Yonsei University

The Effect of Phosphodiesterase inhibitor on browning of adipose tissue in mice model

Directed by Professor Bong-Soo Cha

Doctoral Dissertation
submitted to the Department of Medicine,
the Graduate School of Yonsei University
in partial fulfillment of the requirements for the degree
of Doctor of Philosophy

Da Hea Seo

December 2020

This certifies that the Doctoral Dissertation of Da Hea Seo is approved.

Thesis Supervisor: Bong-Soo Cha

Thesis Committee Member#1: Jae-woo Kim

Thesis Committee Member#2: Ki Taek Nam

Thesis Committee Member#3: Se-Eun Park

Thesis Committee Member#4: Yong-ho Lee

The Graduate School
Yonsei University

December 2020

ACKNOWLEDGEMENTS

I would like to express my gratitude and appreciation for Professor Bong Soo Cha whose guidance, support and encouragement has been invaluable throughout this study. I also wish to thank Professors Jea-woo Kim, Ki Taek Nam, Se Eun Park and Yong-ho Lee who have been a great source of support.

And my biggest thanks to my family for all the support you have shown me through this research. For my kids, sorry for being even grumpier than normal while I wrote this thesis! And for my husband, Seung Young, thanks for all your support, without which I would have stopped these studies a long time ago. Finally, I would like to thank my parents and mother-in-law for supporting me during the compilation of this dissertation.

I would like to praise and thank God, the almighty, who has granted countless blessing, knowledge, and opportunity, so that I have been finally able to accomplish the thesis.

December, 2020

<TABLE OF CONTENTS>

LIST OF FIGURES

ABSTRACT

The Effect of Phosphodiesterase inhibitor on browning of adipose tissue in mice model

Da Hea Seo

Department of Medicine
The Graduate School, Yonsei University

(Directed by Professor Bong Soo Cha)

Background:

Cilostazol is a selective inhibitor of phosphodiesterase type 3 with therapeutic focus on increasing cAMP, which is very important in the development of the beige phenotype and activation of its thermogenic program in white adipose tissue. In this study, we aimed to investigate the effects of inhibition of phosphodiesterase type 3B (PDE3B) by cilostazol in adipose tissue of high fat diet (HFD)-fed mice.

Methods:

Seven-week-old male C57BL/6J mice were randomly assigned to either the cilostazol group or control groups. The control groups were divided into two groups: CHOW diet group and HFD group. Cilostazol (30mg/kg/day) was administered by mixing it in the food for 16 weeks. Expression of UCP1 and other brown adipocyte markers in adipose tissues including white adipose tissue (WAT) were compared.

Results:

In the HFD-fed cilostazol group, C57BL/6J mice displayed improvements in systemic metabolism including improved glucose tolerance and lipid profile but modest effects on body weight. In

perinephric WAT of cilostazol-treated mice, cAMP/protein kinase A (PKA) signaling pathways are activated, resulting in “browning” phenotype, with a smaller fat deposits, and enhanced mRNA expression of UCP1 and other brown adipocyte markers. Cilostaol also attenuated the HFD-induced impairment of UCP1 mRNA expression in interscapular brown adipose tissues (BAT).

Conclusion:

PDE3B appears to be an important regulator of lipid metabolism, insulin sensitivity, and control of thermogenic programs in adipose tissues. An increase in intracellular cAMP by inhibition of PDE3B with cilostazol treatment promoted browning of visceral WAT and attenuated impairment of BAT activity but rather modest effect on overall body weight.

Key words : cilostazol; white adipose tissue; beige adipose tissue

The Effect of Phosphodiesterase inhibitor on browning of adipose tissue in mice model

Da Hea Seo

Department of Medicine
The Graduate School, Yonsei University

(Directed by Professor Bong Soo Cha)

I. INTRODUCTION

Adipose tissues (AT), which include white adipose tissue (WAT) and brown adipose tissue (BAT), play an essential role in regulating whole-body energy homeostasis (1). Excess expansion of WAT due to positive energy balance and defects in thermogenic gene expression in BAT are associated with obesity and various metabolic diseases (2). It is well established that BAT has a central role in adaptive thermogenesis in rodents throughout their lifespan (3). More recently, BAT has been conclusively identified and shown to be functional in adult humans (4). BAT thermogenesis depends on high mitochondrial content and expression of uncoupling protein 1 (UCP-1), which functions as a mitochondrial proton leak, thereby generating heat instead of ATP. In humans, BAT is found in small volumes, where older and obese individuals often have negligible amounts of BAT (5).

Recent studies reveal the presence of a subset of cells in WAT that could be induced by environmental or hormonal factors to become “brown-like” cells, and this “beigeing” process has been suggested to have strong anti-obesity and antidiabetic benefits in animals (6). Indeed, it has recently been shown that

human pre-adipocytes can be differentiated into beige adipocytes in vitro (7). In addition, it has previously been shown that reduced insulin sensitivity is associated with reduced expression of transcripts involved in BAT adipogenesis within subcutaneous WAT in humans (8). When exposed to cold, there is an increase of catecholamine release which then binds to adrenergic receptor on BAT/beige adipose tissue and activates adenylyl cyclase to increase intracellular concentration of cyclic adenosine monophosphate (cAMP), which in turn activates cascade of protein kinase A (PKA) dependent signaling pathway (9). cAMP/PKA signaling pathways play a critical role in differentiation of WAT and BAT and regulation of energy homeostasis (9). Therefore, it would be very important to maintain intracellular level of cAMP in browning of WAT.

Phosphodiesterase (PDE) plays a specific role in hydrolyzing cyclic guanosine monophosphate (cGMP) or cAMP and consists of 11 difference protein groups (10). Among those, there are two form of PDE III (PDE3), which are PDE3A and PDE3B. PDE3A is mainly located in platelet, trachea and cardiovascular tissues while PDE3B is located in organs involved in energy metabolism such as liver, pancreatic beta cells and adipose tissues. In an animal study with PDE3B knockout (KO) mice, epididymal WAT "browning" phenotype, with smaller increases in body weight under high-fat diet, smaller fat deposits (11). Cilostazol, a selective inhibitor of phosphodiesterase III inhibitor, has been approved for the treatment of intermittent claudication and it is known to elevate the intracellular level of cAMP by inhibiting its degradation (12).

In this study, we hypothesized that administration of cilostazol may induce browning of white adipose tissue and improve metabolic parameters.

II. MATERIALS AND METHODS

1. Animal study

Seven-week-old male C57BL/6 mice were housed under standard conditions (21 ± 2˚C, 60 ± 10% humidity, 12 h light/dark cycle) with ad libitum access to food and water. The mice were randomly assigned to either the cilostazol group (n=15) or control groups (n=15) at 7 weeks of age. The control groups were divided into two groups: CHOW diet group (n=5) and high fat diet (HFD; 60 Kcal%) group (n=10). The cilostazol group was fed a HFD (60 Kcal%) containing cilostazol (30 mg/kg/day). The total observation period was 16 weeks. Daily weight, dietary intake, activity patterns, and health status were monitored throughout the experiment.

All animal procedures were performed in accordance with the guidelines of the National Institutes of Health and pre-approved by the animal care and use committee of Yonsei University, College of Medicine (2017-0019).

A. Oral glucose tolerance test (OGTT) and Insulin tolerance test (ITT)

Oral glucose tolerance test (OGTT) was performed after 16 weeks of drug administration. After fasting for 18 hours, 2 g/kg of glucose was administered orally, and blood glucose levels were measured from caudal venous blood using a portable blood glucose meter (Boehringer-Mannheim, Indianapolis, IN, USA) at 0, 15, 30, 60, 90, and 120 minutes post glucose administration.

Insulin tolerance test (ITT) was performed after 16 weeks of drug administration. After fasting for 4 hours, 1 U/kg of insulin (Sigma-Aldrich, Cat. No. 9177C) was administered intraperitoneally, and blood glucose levels from caudal venous blood were measured by a portable blood glucose meter at 0, 15, 30, 60, 90, and 120 minutes post insulin administration.

B. Blood and tissue sampling

After OGTT, after 18 hours of fasting, anesthesia was performed, using a nose cone. Blood was obtained from the abdominal aorta by thoracotomy. The mice were then euthanized. The blood was centrifuged for 10 minutes and the serum was stored at -80 ℃. Post euthanasia, the liver and fat tissue were excised. The liver and fat tissue samples were rapidly frozen with nitrogen solution and stored at -80 ℃. Some liver and fat tissue samples were fixed in 4% paraformaldehyde (Tech & Innovation Co., Ltd., Cat. No. BPP-9004-004LR) solution for more than 48 hours and used for histological analysis.

C. Measurement of serum metabolic parameters

Blood glucose concentrations were measured using an Accu-Chek Performa glucometer (Boehringer-Mannheim, Indianapolis, IN, USA). As prescribed, random blood glucose levels were measured from tail blood in the random-fed (nonfasting) state, at 14:00 using the glucometer. The serum insulin concentrations were determined using enzyme-linked immunosorbent assay (Mouse Insulin ELISA Kit, Merck Millipore, Darmstadt, Germany). Serum aspartate aminotransferase (AST), alanine aminotransferase (ALT), total cholesterol, and triglyceride were also determined.

D. Hematoxylin and eosin (H&E) and immunohistochemical analyses

Tissue samples (AT and liver) were washed, dehydrated, and embedded in paraffin. Some were stained with hematoxylin and eosin (H&E) for observation of histological structures. Sections of adipose tissues were stained with anti-UCP1 antibody (ab10983, Abcam, Cambridge, UK). Tissue samples were examined under a microscope and images were acquired using an attached digital camera. CellSens Entry software

(Olympus, Tokyo, Japan) was used for image analysis.

E. Measurement of adipocyte size and number

Adipocyte diameter, area and total adipocyte number from 3 to 5 AT sections per mouse stained with H&E and imaged at × 100 magnification were quantified by Adiposoft software 1.13.

2. Cell culture and differentiation

The effect of cilostazol on the browning of adipocytes was compared. The 3T3-L1 mouse preadipocyte cell lines were cultured as previously described. In brief, 2-day post-confluent cells (day 0) were cultured in Dulbecco's modified Eagle's medium supplemented with 10% fetal bovine serum, 2 μg ml − 1 dexamethasone, 0.5 mM isobutyl-1-methylxanthine and 1 μg ml − 1 insulin for 2 days. Maturation medium containing fresh Dulbecco's modified Eagle's medium supplemented with 10% fetal bovine serum and 1 μg ml − 1 insulin was changed every 2 days. Fully differentiated adipocytes were used for experiments after 7 days. During the 7-day differentiation process, cells in complete medium were treated with or without cilostazol for 4 hours and then harvested.

The immortalized brown adipocyte precursor cells were cultured under 5% CO2 at 37 ℃ in high-glucose Dulbecco's modified Eagle's medium (Wel-GENE Inc., Daegu, Korea) supplemented with 10% fetal bovine serum (Wel-GENE Inc.), 1% penicillin and 1% streptomycin (Gibco, Life Technologies, Grand Island, NY, USA).27 On day 1, the medium was changed to induction medium containing 20 nM insulin, 1 nM T3 (Sigma-Aldrich, St Louis, MO, USA), 0.5 μM isobutyl-1-methylxanthine (Sigma-Aldrich), and 0.125 mM indomethacin (Sigma-Aldrich). Two days after induction, cells were switched to the maintenance medium containing 20 nM insulin (Roche, Mannheim, Germany) and 1 nM T3 that was changed

every day thereafter. The cells were harvested on day 7.

A. RNA isolation and reverse transcriptase-polymerase chain reaction (RT–PCR) analysis

Total RNA was isolated from cells with TRIzol reagent (Invitrogen, Carlsbad, CA, USA) following the manufacturer's instructions, and then complementary DNA (cDNA) was synthesized using the High Capacity cDNA Reverse Transcription kit (Applied Biosystems, Foster City, CA, USA). The cDNA was then amplified in the ABI 7500 sequence detection system (Applied Biosystems) using Power SYBR Green PCR Master Mix (Applied Biosystems) with the following cycling conditions: 40 cycles at 95 ℃ for 5 s, 58 ℃ for 10 s and 72 ℃ for 20 s. All experiments were performed at least in triplicate and target gene expression was normalized to glyceraldehyde 3-phosphate dehydrogenase (Gapdh) mRNA. Quantitative analyses were conducted using the ΔΔcycle threshold method and StepOne Software, version 2.2.2 (Applied Biosystems, Waltham, MA, USA).

B. Western blot.

Homogenized adipose tissue was lysed in RIPA buffer containing protease and phosphatase inhibitors. After separated on sodium dodecyl sulphate-polyacrylamide gel electrophoresis (SDSPAGE) the proteins were electroblotted to polyvinylidene fluorid (Millipore Billerica, USA). The membranes were blocked an incubated with different antibodies, then incubated with secondary antibodies. The blots were visualized by enhanced chemiluminescenc reagents (Amersham Pharmacia Uppsala, Sweden) according to the manufacturer's protocol. The immunoreactive band was quantified using ImageJ 4.1 software (NIH, Bethesda MD, USA).

3. Statistical analysis

Outcomes were compared using the Wilcoxon-Mann-Whitney U test to determine the differences between continuous variables. To compare continuous variables, patient characteristics were analyzed using the Kruskal-Wallis test, and categorical variables were compared using the $\chi 2$ test, followed by post hoc analyses using the Dunn procedure for Kruskal-Wallis test.

Statistical analyses were performed using IBM SPSS statistical software for Windows, version 25.0 (IBM, Armonk, NY, USA). A p value < 0.05 was considered statistically significant.

III. RESULTS

1. Oral administration of cilostazol had modest effects on body weight but displayed the beige phenotype in the visceral WAT in HFD mice

Given the potential clinical relevance of cAMP in understanding mechanisms for induction of BAT in WAT depots, 7-weeks old male C57BL6 mice were fed with HFD to induce diet-induced obesity with or without cilostazol. The body weight of the both cilostazol-treated and HFD control mice were significantly greater than that of the matched CHOW control mice (Fig. 1A). The cilostazol treatment only had the modest effect on the overall body weight (Fig. 1A), food intake (Fig. 1B) and random blood glucose levels (Fig. 1C) compared to the HFD control mice. However, the gross size and overall weight of perinephric (visceral) WAT and interscapular BAT from cilostazol-treated mice was markedly smaller than that of HFD control mice (Fig. 1D and 1F) while the weight of inguinal (subcutaneous) WAT was higher in cilostazol-treated than HFD control mice (Fig 1E).

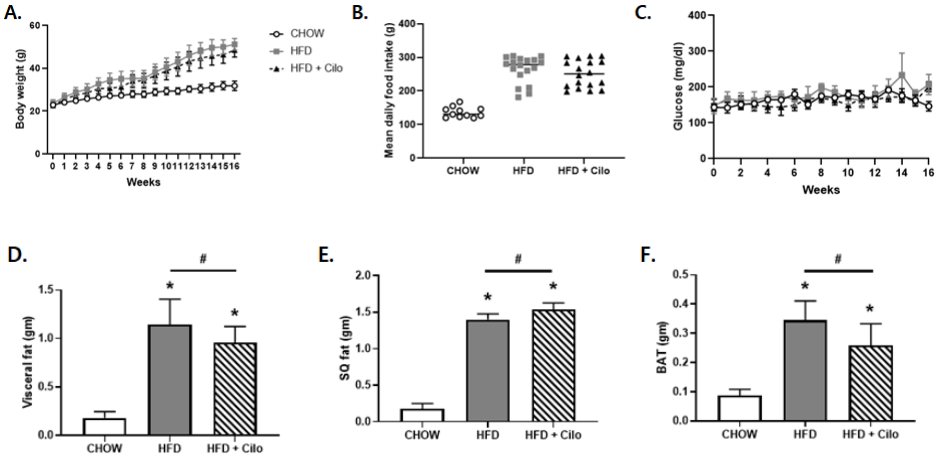

Figure 1. Cilostazol treatment had modest effect on body weight with HFD-induced obesity but modified adipose tissue. A. Change in body weight, **B.** Average food intake per day, **C.** Changes in the mean random glucose levels during 16 weeks of experiment, **D.** Changes in visceral (perinephric) fat weight, **E.** Changes in subcutaneous fat (SQ) weight, **F.** Changes in interscapular brown adipose tissue (BAT) weight. Error bars represent standard error of mean. *$p < 0.05$ versus corresponding CHOW control value and # $p < 0.05$ versus corresponding HFD control value. HFD, high fat diet.

We further examined the role of cilostazol on the size of adipocytes and found that administration of cilostazol resulted in significantly smaller diameters of visceral white adipocytes (Fig. 2A and 2B). No significant differences in the size of subcutaneous white adipocytes (Fig 2C and 2D).

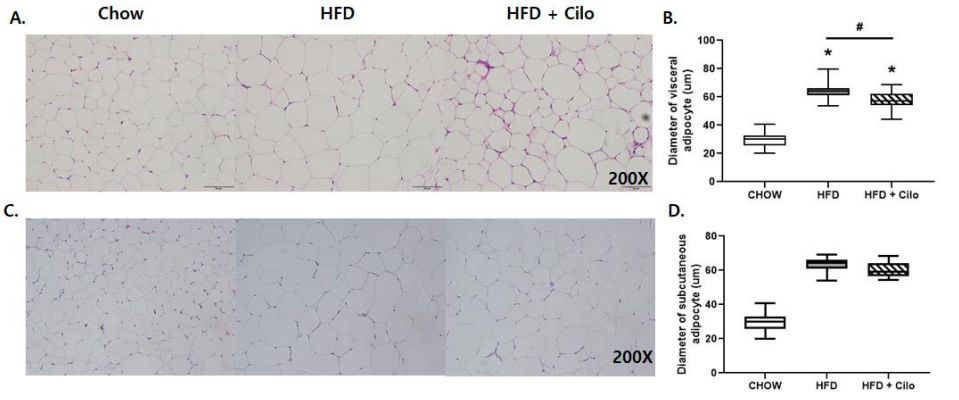

Figure 2. Cilostazol treatment reduced the size of adipocytes in visceral adipose tissue only. A. Representative histological images of H&E stained visceral white adipose tissue section (magnification, x200) of CHOW control, HFD control and cilostazol-treated mice respectively **B.** Adipocyte diameters of visceral adipocyte tissue from CHOW control, HFD control and cilostazol-treated mice. **C**. Representative histological images of H&E stained subcutaneous white adipose tissue section (magnification, x200) of CHOW control, HFD control and cilostazol-treated mice respectively **D.** Adipocyte diameters of subcutaneous adipocyte tissue from CHOW control, HFD control and cilostazol-treated mice.*$p < 0.05$ versus corresponding CHOW control value and # $p < 0.05$ versus corresponding HFD control value. HFD, high fat diet.

2. Cilostzol improved glycemic index in HFD mice

During 16 weeks of cilostazol treatment, these were no significant differences in the mean random glucose levels between HFD groups (Fig. 1C). However, OGTT results showed that the cilostazol group exhibited significant improvement in glucose tolerance 30, 60, 90 and 120 minutes after glucose administration, compared with the HFD control group (Figures 3A). The AUC value of OGTT was significantly lower for the cilostazol group than the

HFD control group (Figures 3B).

For ITT, cilostazol group displayed a nonsignificant trend of improvement in glucose levels compared with the HFD control group (Fig. 3C). However, the differences in AUC value of ITT was marginally significant (p=0.051) between HFD groups (control vs cilostazol) (Fig. 3D).

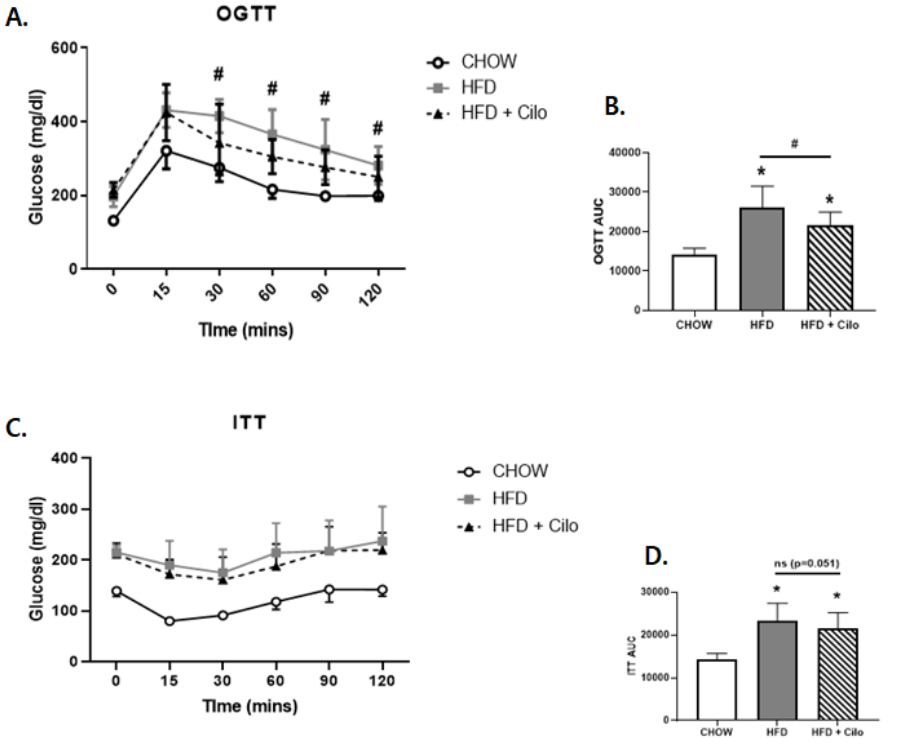

Figure 3. Cilostzol improved glycemic index. A. Oral glucose tolerance test, **B.** Differences in the AUC of oral glucose tolerance test, **C.** Insulin tolerance test, **D.** Differences in the AUC of insulin tolerance test. *p < 0.05 versus corresponding CHOW control value and # p < 0.05 versus corresponding HFD control value. AUC, area under the curve; HFD, high fat diet.

3. Cilostazol increased brown adipocyte maker gene expressions in visceral WAT isolated from cilostazol-treated HFD mice

To address whether cilostazol promoted WAT browning, we performed UCP1 immunohistochemistry staining, which demonstrated enhanced UCP1 signals in visceral WAT of cilostazol treated HFD mice (Fig. 4A) while no differences were noted in subcutaneous WAT (Fig. 4B).

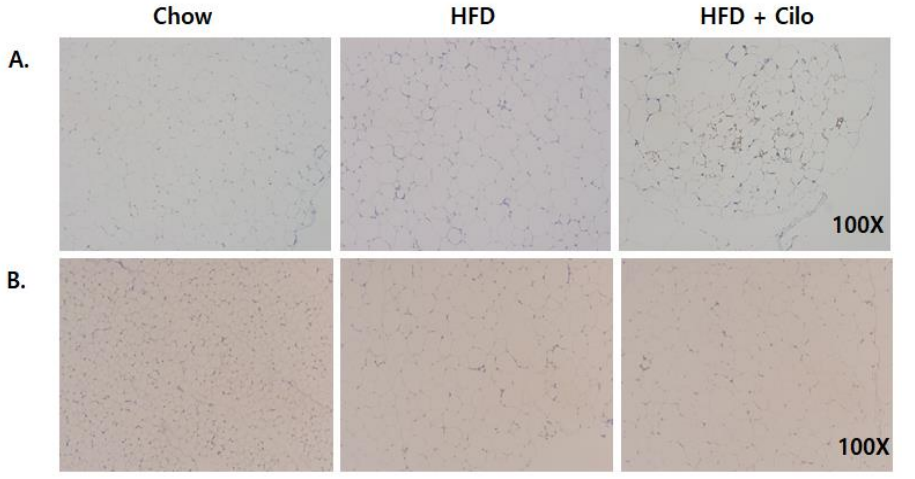

Figure 4. Cilostazol induced browning of WAT. A. Representative histological images of UCP1 immunohistochemical stained (brown) visceral WAT section (magnification, x100) of CHOW control, HFD control and cilostazol-treated mice **B.** Representative histological images UCP1 immunohistochemical stained (brown) subcutaneous WAT section (magnification, x100) of CHOW control, HFD control and cilostazol-treated mice. WAT, white adipose tissue.

Moreover, administration of cilostazol upregulated mRNA expression of UCP1, PGC1α, PRDM16, CPT2, DIO2 and CIDEA in visceral WAT, suggesting that inhibition of PDE3B with cilostazol promoted thermogenesis, mitochondrial biogenesis, and fatty acid oxidation programs even in HFD mice (Fig 5A-F). But cilostazol treatment did not affect the expression of UCP1 in subcutaneous WAT (Fig 6).

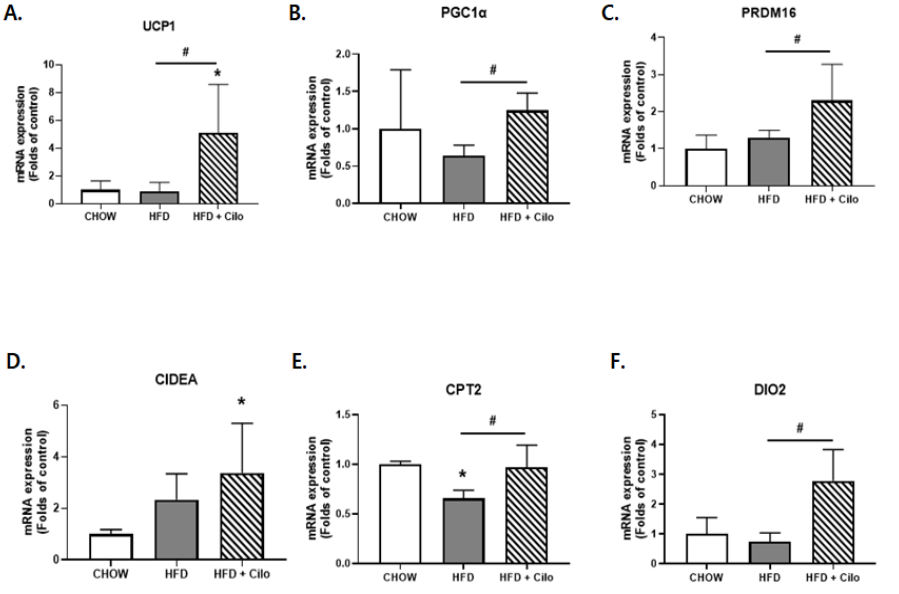

Figure 5. Cilostazol increased the expression of genes related to browning of visceral WAT. A-F. RT-PCR analysis of brown adipocyte marker genes in visceral adipose tissue. *p < 0.05 versus corresponding CHOW control value and # p < 0.05 versus corresponding HFD control value. HFD, high fat diet.

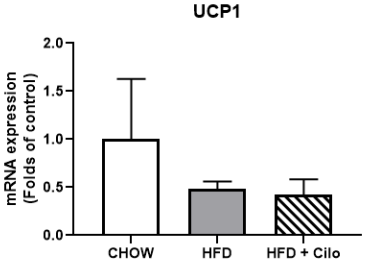

Figure 6. Cilostazol did not affect the expression of UCP1 in subcutaneous WAT. RT-PCR analysis of UCP1 in subcutaneous adipose tissue.

4. Cilostazol attenuated HFD-induced accumulation of large lipid droplets in BAT and HFD-induced impairment of BAT activity

To determine whether cilostazol affected BAT, interscapular BAT was examined. While overall amount of BAT was significantly higher in both HFD mice groups compared to CHOW control group (Fig. 1F), cilostazol attenuated HFD-induced accumulation of unilocular large lipid droplets within brown adipocytes. In other words, multilocular lipid droplets identified by H&E staining and UCP1-positive appearance were comparable between cilostazol-treated HFD group and HFD control group (Fig. 6A and 6B). Moreover, cilostazol significantly attenuated HFD-induced impairment of BAT activities, assessed by mRNA expression of UCP1, PGC1α, PRDM16, CPT2, DIO2 and CIDEA, key transcriptional regulators of thermogenesis in BAT (Fig. 7A-F).

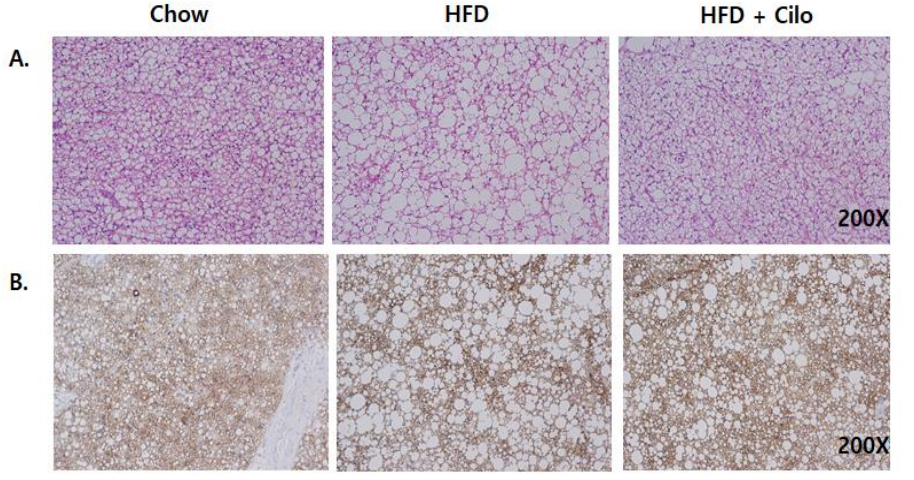

Figure 7. Cilostazol treatment attenuated HFD-induced accumulation of unilocular large lipid droplets accumulation within brown adipocytes. A. Representative histological images of H&E- stained BAT section (magnification, x200), **B.** Representative histological images of UCP1

immunohistochemical stained (brown) BAT section (magnification, x200) of CHOW control, HFD control and cilostazol-treated mice. *p < 0.05 versus corresponding CHOW control value and # p < 0.05 versus corresponding HFD control value. BAT, brown adipose tissue; HFD, high fat diet.

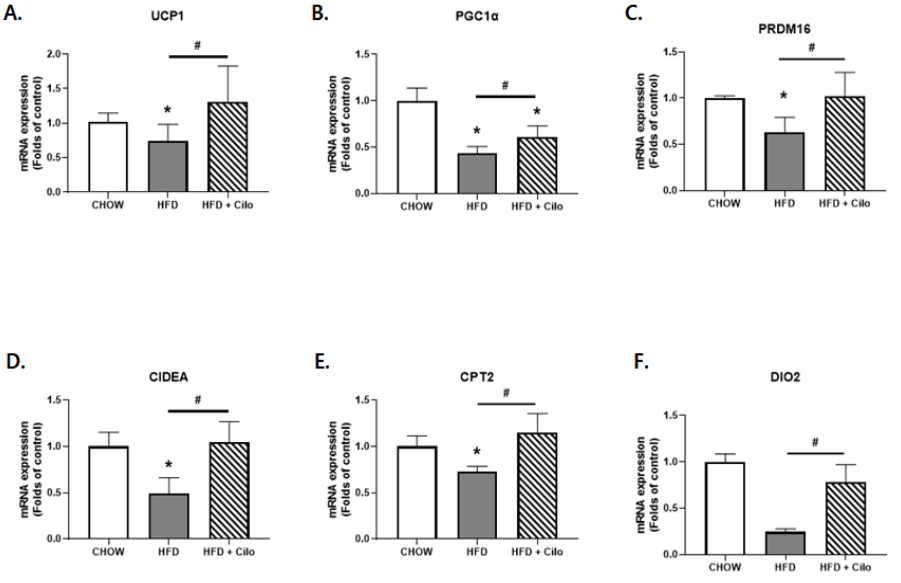

Figure 8. Cilostazol stimulated expressions of brown adipogenic and thermogenic transcriptional factors. A-F. RT-PCR analysis of brown adipocyte marker genes in brown adipose tissue. *p < 0.05 versus corresponding CHOW control value and # p < 0.05 versus corresponding HFD control value. HFD, high fat diet.

5. Cilostazol increased brown adipocyte marker gene expressions in 3T3-L1 adipocytes

A regulatory role for PDE3B in induction of UCP1 in cilostazol-treated HFD mice of visceral WAT was confirmed in fully 3T3-L1 adipocytes. Incubation of differentiated 3T3-L1 adipocytes with cilostazol amplified the

expression of UCP1, which was replicated by dibutyryl cyclic adenosine monophosphate (dbcAMP), a cAMP analogue (Fig. 8A and 8B). Similarly, intracellular cAMP levels were also increased with either treatment with cilostazol or dbcAMP (Fig. 8C). Furthermore, the expression of BAT related genes such as PRDM16, PGC1α, CIDEA and CPT2 were also enhanced in cilostazol-treated 3T3-L1 adipocytes (Fig. 8D-I).

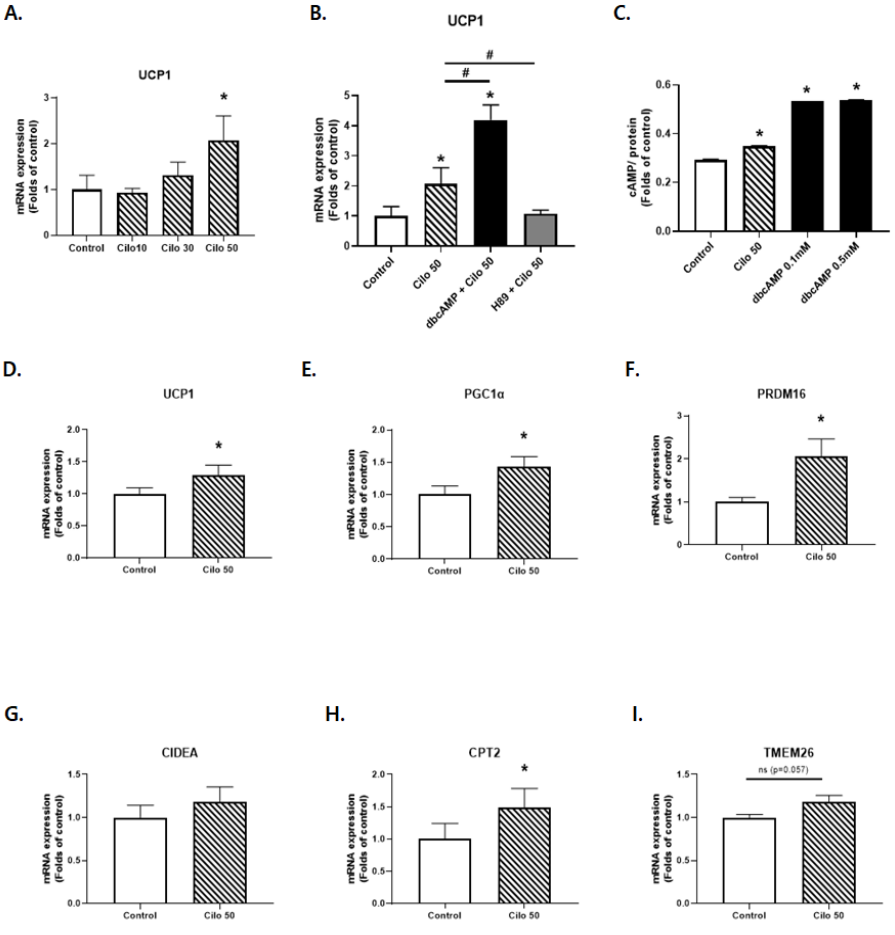

Figure 9. Cilostazol increased intracellular cAMP concentration and UCP1 expression in 3T3L1 adipocytes. A. Dose dependent qPCR analysis

of UCP1 after cilostazol treatment in 3T3L1 adipocytes. **B.** qPCR analysis of UCP1 after PKA inhibition by H89 in 3T3-L1 adipocytes. Cilostazole or dbcAMP were treated for 4h, **C.** Intracellular cAMP levels in control, cilostazol-treated, dbcAMP-treated and cilostazol and dbcAMP-treated 3T3L1 adipocytes. **D-I.** qPCR analysis of other brown adipocytes marker genes. *p < 0.05 versus corresponding control value.

6. Cilostazol-treated brown adipocytes showed increased expression of thermogenic transcriptional factors

Cilostazol promoted elevation of intracellular cAMP levels in brown adipocytes (Fig. 9A). Furthermore cilostazol upregulated UCP1, PRDM16, and PGC1α mRNA expression, key transcriptional regulators of thermogenesis in brown adipocytes (Fig. 9B-D).

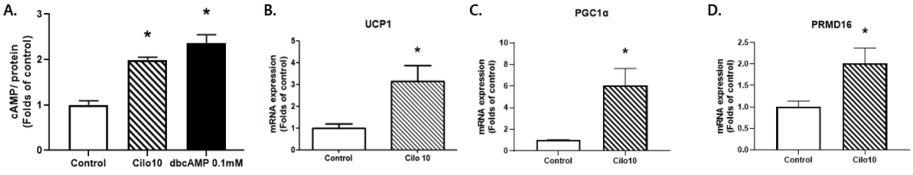

Figure 10. Cilostazol increased intracellular cAMP concentration and UCP1 expression in immortalized brown adipocytes. A. cAMP levels in control, cilostazol-treated and dbcAMP-treated immortalized brown adipocytes. **B-D.** qPCR analysis of UCP1 and other brown adipocytes marker genes. *p < 0.05 versus corresponding control value.

7. Cilostazol may induce adipocyte browning through activation of AMPK via increased intracellular cAMP

AMPK is well-known to play a role in promoting WAT browning and cAMP/PKA signaling has been proved to be a potent AMPK activator. So we

supposed that cilostazol may stimulate WAT browning through activation of AMPK. To explore the potential mechanism of cilostazol-induced browning in WAT and UCP1 upregulation, fully differentiated 3T3-L1 adipocytes were treated with cilostazol and PKA inhibitor, H89. While cilostazol alone amplified the mRNA expression of UCP1, the induction of UCP1 by cilostazol was inhibited by H89 (Fig. 8B). As seen in Fig. 10A and 10B, inhibition of PDE3B with cilostazol increased phosphorylation of AMPK, which was inhibited by H89.

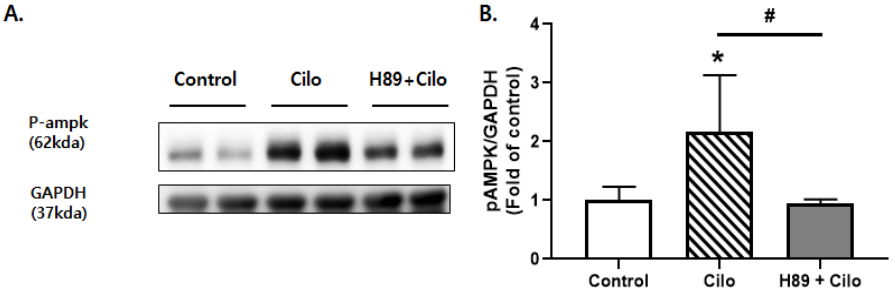

Figure 11. Cilostazol may induce adipocyte browning through activation of AMPK. A. Immunoblot analysis of 3T3L1 adipocytes after cilostazol treatment with or without PKA inhibition by H89. **B.** Ratios of pAMPK/GAPDH are presented as bar graphs.

8. Cilostazol attenuated HFD-induced hepatic steatosis

Observation of livers of the mice showed that cilostazol treatment attenuated HFD-induced accumulation of lipids in the liver. Cilostazol treatment for 16 weeks significantly attenuated HFD-induced increase in liver weight (Fig. 11A). While plasma total cholesterol (TC), triglyceride (TG), AST (aspartate aminotransferase) and alanine aminotransferase (ALT) levels were increased in HFD mice compared to CHOW mice, cilostazol

treatment reversed the increase in plasma TC, TG, AST and ALT levels induced by the HFD (Fig. 11C-E). Moreover, cilostazol reduced hepatic TG contents, which was comparable to control HFD mice (Fig. 11F).

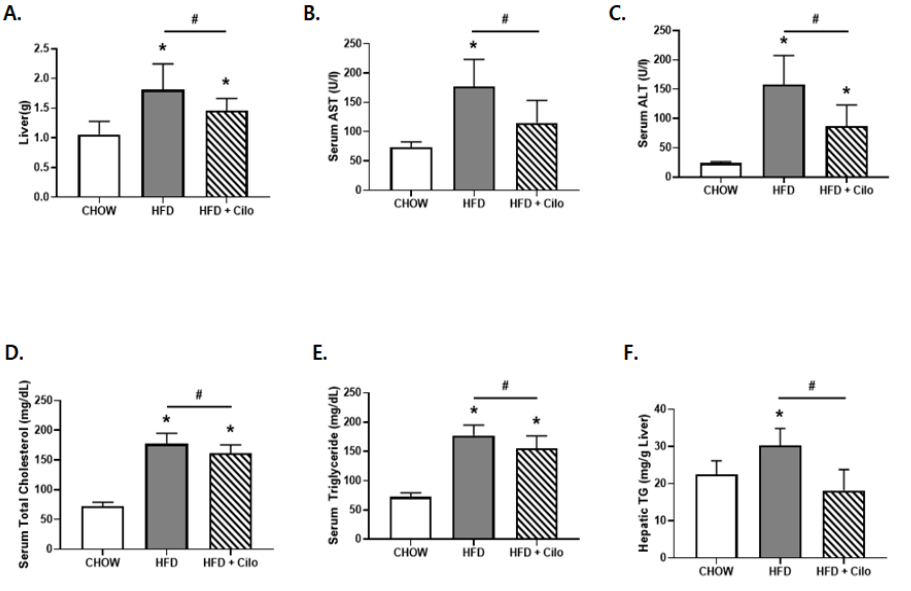

Figure 12. Effects of cilostazol on aspartate aminotransferase and alanine aminotransferase levels and hepatic triglyceride level. A. Change in overall liver weight, **B.** AST level (IU/L), **C.** ALT level (IU/L), **D.** Serum total cholesterol level (mg/dL), **E.** Serum triglyceride level (mg/dL), **F.** Hepatic triglyceride (mM/g). Error bars represent standard error of mean. *p < 0.05 versus corresponding CHOW control value and # p < 0.05 versus corresponding AST; aspartate aminotransferase, IU/L; international units per liter, ALT; alanine aminotransferase; HFD control value. HFD, high fat diet.

Liver histology by H&E staining showed that cilostazol treatment markedly attenuated HFD-induced aberrant lipid accumulation (Fig. 12A). HFD-induced increase of the expression level of MCP-1, αSMA and COLA1 which are markers of hepatic stellate cell activation was significantly

reversed by cilostazol treatment (Fig. 12B-D).

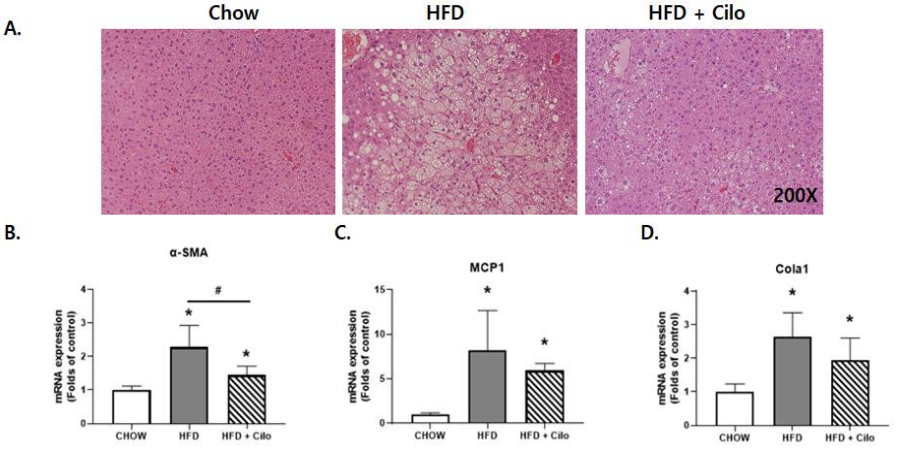

Figure 13. Cilostazol improved hepatic steatosis with reduced expression of MCP-1, αSMA and COLA1 in hepatocytes of HFD mice. A. Representative histological images of H&E- stained liver section (magnification, x200) of CHOW control, HFD control and HFD cilostazol-treated mice, **B.** qPCR analysis of MCP1, **C.** qPCR analysis of αSMA, **D.** qPCR analysis of COLA1. $p < 0.05$ versus corresponding CHOW control value and # $p < 0.05$ versus corresponding HFD control value. HFD, high fat diet

IV. DISCUSSION

White adipose browning, a process that transforms energy-storing white adipocytes into heat-producing beige adipocytes in WAT, represents an attractive strategy to increase energy expenditure and treat obesity and diabetes. Discovering compounds with WAT browning effects is therefore of great importance to provide alternative approaches for the treatment of these common but serious conditions. Previous studies demonstrated that PDE3B KO mice acquired characteristics of a beige phenotype, including changes in

morphology, increased expression of genes related to recruitment of beige adipocytes, increased UCP1 and energy dissipation (11). In this work, we presented clear data supporting a function of PDE3B inhibition in raising energy expenditure by promoting WAT browning and provide the possibility into the therapeutic effects of cilostazol on obesity and obesity-related complications such as hepatic steatosis.

In this study, cilostazol treatment resulted in an improved glycemic index, including significant reductions in glucose tolerance and marginally significant improvement in insulin sensitivity. Cilostazol treatment also significantly decreased the size of fat pads and adipocytes of visceral WAT. Moreover, cilostazol treatment resulted in activation of several genes crucial for BAT such as PRDM16, PGC1α, ELOVL3, CIDEA and CPT2 in both visceral WAT and interscapular BAT of HFD mice as well as 3T3L1 adipocytes and brown adipocytes. However, changes in body weight were rather modest, suggesting that it may require some additional stimuli to induce more functional brown adipocyte differentiation.

Cilostazol is an antiplatelet drug that inhibits both primary and secondary platelet aggregation in response to ADP, collagen, epinephrine, and arachidonic acid (12). The antiplatelet and vasodilator properties of cilostazol are attributed to its ability to elevate intracellular levels of cAMP via inhibition of cAMP phosphodiesterase. Cilostazol has been approved for the treatment of intermittent claudication. Furthermore, there have been evidences supporting the role of PDE inhibition for improvements in systemic metabolism. Human studies demonstrated a beneficial effect of cilostazol on lipoprotein metabolism characterized by an increase in high-density lipoprotein-cholesterol and a reduction of plasma triglyceride levels (13, 14). Moreover, cilostazol treatment has shown improvement in insulin resistance in

diabetic rat models (15, 16). However, pharmacological efficacy of cilostazol in obesity has not yet been investigated.

cAMP is very important in the development of the beige phenotype and activation of its thermogenic program (17). As seen in Fig 8C and 10A, the inhibition of PDE3B by cilostazol treatment increased intracellular concentration cAMP with subsequent AMPK signaling, the integration of which resulted in upregulation of PGC1α and induction of PRDM16. In other words, in visceral WAT of cilostazol treated HFD mice, PRDM16 initiated a coordinated metabolic program by upregulating PGC-1α, ELOVL3, CIDEA, and DIO2, and critical mitochondrial proteins, including UCP1 and CPT2 which might be responsible for increased thermogenesis. In 3T3-L1 adipocytes, down-regulation of PDE3B, via pharmacologic inhibition with cilostazol also increased intracellular concentration cAMP with subsequent AMPK signaling resulting in activation of PGC-1α and enhanced induction of UCP1 mRNA. Thus, we suggest that, PDE3B may regulate a cAMP-sensitive molecular "switch" for "browning" of visceral WAT. It is also noteworthy to mention that cilostazol treatment was associated with an increase in subcutaneous WAT while the visceral WAT was reduced. This indicates that cilostazol treatment may be associated with adipose tissue remodeling and redistribution, which may account for the improved lipid profiles and hepatic steatosis.

Our data support the idea that increased cAMP signaling in cilostazol-treated mice leads to activation of AMPK-signaling. Studies in 3T3L1 adipocytes indicated that cilostazol increased phosphorylation of AMPK, suggesting that PDE3B regulated a cAMP "pool" importation in regulation of AMPK. AMPK is a key regulator of energy metabolism and mitochondrial biogenesis (18). The promotive effects of AMPK on WAT browning and BAT activity have been extensively investigated (18). It was reported that the modulatory

function of myostatin, adiponectin and irisin on WAT browning involve AMPK activation (19-21). Experiments with 3T3L1 adipocytes showed that browning-promotive effects of cilostazol were substantially abolished by the treatment with H89, a PKA inhibitor, suggesting a regulatory role of cAMP and PKA as well as AMPK signaling. Although further investigation such as animal experiments using systemic or adipose-specific AMPK KO mice are still needed to prove that AMPK is the cause of fat browning in vivo, the current data provide an important hint that AMPK activation may involve the cilostazol induced WAT browning at least in vitro.

Beige and brown adipocytes are recognized as having a potential role in the defense against obesity by dissipating energy. Variation in the activation and amount of BAT may regulate energy expenditure, but BAT is inversely correlated with body weight and decreases with age (3). In the present study, the amount of interscapular BAT was reduced in cilostazol-treated HFD mice compared to control HFD mice however, the levels of UCP1 mRNA and morphologic assessment of numerous unilocular lipid droplets were comparable between interscapular BAT from HFD control and cilostazol-treated mice. It appears that cilostazol attenuated HFD-induced lipid accumulation in BAT and impairment of BAT activity. In fact, the use of cilostazol increased intracellular concentration of cAMP in brown adipocytes, which stimulated expressions of thermogenic and brown-specific genes, enhancing its metabolic activity as demonstrated in our study.

The WAT is divided into two main types, visceral and subcutaneousWAT, which show differences in gene expression, metabolic profile, and cell composition (22). The visceral WAT is known to be more resistant to acquire a thermogenic profile than subcutaneous WAT (23). However, in our study, the effect of cilostazol was only apparent in visceral WAT while minimal changes

were noted in subcutaneous WAT. Although further studies are warranted to explain these interesting findings, we can speculate from a study where the alteration in activity and expression of cyclic nucleotide PDE families in omental and subcutaneous adipose tissue and adipocytes in obese humans (24). There were inverse correlations between BMI and PDE3 activities in isolated adipocytes from omental WAT, while no correlation was found in subcutaneous WAT of obese subjects (24).

There are several limitations of this study. First, administration of cilostazol was admixed, of which dosing technique may not be reliable in all animals. Instead, injection of cilostazol into the peritoneal cavity may have been more ideal technique in this setting, however, intraperitoneal delivery may induce painful ileus and peritonitis in rodents, with subsequent adhesions (25). Second, the mouse study populations were not large enough for several analyses. For this reason, we cannot exclude the possibility that the statistically insignificant results in this study may still have clinical significance. Third, although we have provided the evidence for amelioration of hepatic steatosis with cilostazol treatment, we were not able to provide the underlying mechanism, which may need further investigation.

V. CONCLUSION

The use of cilostazol promoted beigeing of visceral WAT, increased activity of BAT and improved glycemic index and hepatic steatosis. Collectively, our data indicate that cilostazol is able to exert multiple beneficial effects through both white and brown adipocytes and may serve as a therapeutic target in obese patients with diabetes.

REFERENCES

1. Harms M, Seale P. Brown and beige fat: development, function and therapeutic potential. Nat Med. 2013;19(10):1252-63.
2. Lowell BB, Spiegelman BM. Towards a molecular understanding of adaptive thermogenesis. Nature. 2000;404(6778):652-60.
3. Cannon B, Nedergaard J. Brown adipose tissue: function and physiological significance. Physiol Rev. 2004;84(1):277-359.
4. Cypess AM, Lehman S, Williams G, Tal I, Rodman D, Goldfine AB, et al. Identification and importance of brown adipose tissue in adult humans. N Engl J Med. 2009;360(15):1509-17.
5. Wang Q, Zhang M, Ning G, Gu W, Su T, Xu M, et al. Brown adipose tissue in humans is activated by elevated plasma catecholamines levels and is inversely related to central obesity. PLoS One. 2011;6(6):e21006.
6. Seale P, Bjork B, Yang W, Kajimura S, Chin S, Kuang S, et al. PRDM16 controls a brown fat/skeletal muscle switch. Nature. 2008;454(7207):961-7.
7. Carey AL, Vorlander C, Reddy-Luthmoodoo M, Natoli AK, Formosa MF, Bertovic DA, et al. Reduced UCP-1 content in in vitro differentiated beige/brite adipocytes derived from preadipocytes of human subcutaneous white adipose tissues in obesity. PLoS One. 2014;9(3):e91997.
8. Yang X, Enerbäck S, Smith U. Reduced expression of FOXC2 and brown adipogenic genes in human subjects with insulin resistance. Obes Res. 2003;11(10):1182-91.
9. Ramseyer VD, Granneman JG. Adrenergic regulation of cellular plasticity in brown, beige/brite and white adipose tissues. Adipocyte. 2016;5(2):119-29.
10. Keravis T, Lugnier C. Cyclic nucleotide phosphodiesterase (PDE) isozymes as targets of the intracellular signalling network: benefits of PDE inhibitors in various diseases and perspectives for future therapeutic developments. Br J Pharmacol. 2012;165(5):1288-305.
11. Chung YW, Ahmad F, Tang Y, Hockman SC, Kee HJ, Berger K, et al.

White to beige conversion in PDE3B KO adipose tissue through activation of AMPK signaling and mitochondrial function. Sci Rep. 2017;7:40445.

12. Goto S. Cilostazol: potential mechanism of action for antithrombotic effects accompanied by a low rate of bleeding. Atheroscler Suppl. 2005;6(4):3-11.

13. Nakamura N, Hamazaki T, Johkaji H, Minami S, Yamazaki K, Satoh A, et al. Effects of cilostazol on serum lipid concentrations and plasma fatty acid composition in type 2 diabetic patients with peripheral vascular disease. Clin Exp Med. 2003;2(4):180-4.

14. Toyota T, Oikawa S, Abe R, Sano R, Suzuki N, Hisamichi S, et al. Effect of Cilostazol on Lipid, Uric Acid and Glucose Metabolism in Patients with Impaired Glucose Tolerance or Type 2 Diabetes Mellitus. Clinical Drug Investigation. 2001;21(5):325-35.

15. Nakaya Y, Minami A, Sakamoto S, Niwa Y, Ohnaka M, Harada N, et al. Cilostazol, a phosphodiesterase inhibitor, improves insulin sensitivity in the Otsuka Long-Evans Tokushima Fatty Rat, a model of spontaneous NIDDM. Diabetes Obes Metab. 1999;1(1):37-41.

16. Chang SA, Cha BY, Yoo SJ, Ahn YB, Song KH, Han JH, et al. The effect of cilostazol on glucose tolerance and insulin resistance in a rat model of non-insulin dependent diabetes mellitus. Korean J Intern Med. 2001;16(2):87-92.

17. Hansen JB, Kristiansen K. Regulatory circuits controlling white versus brown adipocyte differentiation. Biochem J. 2006;398(2):153-68.

18. Wu L, Zhang L, Li B, Jiang H, Duan Y, Xie Z, et al. AMP-Activated Protein Kinase (AMPK) Regulates Energy Metabolism through Modulating Thermogenesis in Adipose Tissue. Front Physiol. 2018;9:122.

19. Shan T, Liang X, Bi P, Kuang S. Myostatin knockout drives browning of white adipose tissue through activating the AMPK-PGC1α-Fndc5 pathway in muscle. Faseb j. 2013;27(5):1981-9.

20. Hui X, Gu P, Zhang J, Nie T, Pan Y, Wu D, et al. Adiponectin Enhances Cold-Induced Browning of Subcutaneous Adipose Tissue via

Promoting M2 Macrophage Proliferation. Cell Metab. 2015;22(2):279-90.

21. Lee HJ, Lee JO, Kim N, Kim JK, Kim HI, Lee YW, et al. Irisin, a Novel Myokine, Regulates Glucose Uptake in Skeletal Muscle Cells via AMPK. Mol Endocrinol. 2015;29(6):873-81.

22. Macotela Y, Emanuelli B, Mori MA, Gesta S, Schulz TJ, Tseng YH, et al. Intrinsic differences in adipocyte precursor cells from different white fat depots. Diabetes. 2012;61(7):1691-9.

23. Rosen ED, Spiegelman BM. What we talk about when we talk about fat. Cell. 2014;156(1-2):20-44.

24. Omar B, Banke E, Ekelund M, Frederiksen S, Degerman E. Alterations in cyclic nucleotide phosphodiesterase activities in omental and subcutaneous adipose tissues in human obesity. Nutrition & diabetes. 2011;1(8):e13.

25. Gotloib L, Wajsbrot V, Shostak A. A short review of experimental peritoneal sclerosis: from mice to men. Int J Artif Organs. 2005;28(2):97-104.

ABSTRACT(IN KOREAN)

마우스 모델에서 지방조직 갈색화에 대한 Phosphodiesterase inhibitor 의 역할

<지도교수 차 봉 수>

연세대학교 대학원 의학과

서 다 혜

서론:
실로스타졸은 phosphodiesterase type 3의 선택적 억제제로, cAMP를 증가시키는 치료에 초점을 맞추고 있으며, 이는 백색 지방의 베이지색 지방 표현형의 발달과 열발생 프로그램의 활성화에 매우 중요하다. 본 연구에서는 고지방식이 비만 마우스 모델의 지방 조직에서 실로스타졸에 의한 phosphodiesterase type 3B (PDE3B)의 억제 효과를 조사하고자 하였다.

재료 및 방법:
7주령 수컷 C57BL/6J 마우스를 실로스타졸 그룹 또는 대조군에 무작위로 배정하였다. 대조군은 차우 (CHOW) 그룹과 고지방식이 그룹의 두 그룹으로 나누었다. 실로스타졸 (30mg/kg/day)은 16주 동안 음식에 혼합하여 투여했다. 백색 지방 조직을 포함하는 지방 조직에서 UCP1 발현 및 기타 갈색 지방 세포 마커의 발현정도를 비교 하였다.

결과:

고지방식이와 실로스타졸 투약을 병행한 군에서는 고지방식이 대조군에 비해 포도당 내성 및 지질 수치를 포함한 전신 신진대사가 개선되었지만 체중에 미치는 영향은 적었다. 실로스타졸 투약한 마우스의 내장 백색지방에서, cAMP/PKA 신호 전달 경로가 활성화되어 "갈색지방" 표현형, 작은 사이즈의 지방세포 그리고 UCP1을 포함한 다른 갈색 지방 세포 유전자들의 발현이 증가가 관찰되었다. 또한 실로스타졸은 견갑골 갈색 지방 조직에서 발현의 고지방식이로 인한 UCP1 발현의 장애를 감소시켰다.

결론:

PDE3B는 지방 조직에서 지질 대사, 인슐린 감수성 및 열 생성 프로그램의 조절을 조절하는 중요한 역할을 하는 것으로 생각된다. 실로스타졸로 인한 PDE3B의 억제는 세포 내 cAMP의 증가 및 내장 백색지방의 갈색화를 촉진하고 갈색지방의 활성 장애를 감소시켰다.

핵심되는 말 : cilostazol, 백색지방세포, 베이지색지방세포